Nonlinear Behavior of a Passive Zero-Spring-Rate Suspension System

Stanley E. Woodard* and Jerrold M. Housner*
NASA Langley Research Center, Hampton, Virginia 23665

Various concepts for advanced suspension systems have been proposed for counteracting gravity loads in ground vibration testing of large space structures. Approximating the flight modes of a low-frequency flexible structure in a ground test requires a very soft suspension system. The dynamic behavior of a passive zero-spring-rate mechanism, sometimes used for such ground testing, is analyzed. This mechanism reduces the stiffness inherent in suspending a test specimen by cables. However, the mechanism is shown to be sensitive to imperfections. Imperfections can initiate nonlinear behavior, which becomes more pronounced at lower operating frequencies. Furthermore, large pendular motion of the suspension system couples with the vertical motion, producing additional nonlinearity.

Nomenclature

A = beam cross-sectional area
b = length of suspension cable
E = beam elasticity
g = acceleration due to gravity
h = nondimensional total energy
H = total energy
$\bar{h}$ = nondimensional energy parameter
K = linear spring stiffness
K_{cable} = cable stiffness
K_{neg} = stiffness due to prestressed beams
l = beam length
M = mass of cable and specimen
m_{cable} = mass of cable
m_{specimen} = mass of test specimen
P = prestressed load
P_c = critical load
$\bar{P}$ = nondimensional applied load
Q = unbalanced spring force
t = time
$\bar{t}$ = nondimensional time
w = vertical displacement from horizontal beam position
$\bar{w}$ = vertical displacement from equilibrium position
w_{equil} = vertical equilibrium position of motion
ϕ = test article angular displacement
ω_0 = spring-mass frequency
$\omega_{\text{resultant}}$ = resultant frequency with prestressed load
ω_{eff} = effective frequency with cable stiffness considered
η = nondimensional test specimen vertical velocity
ξ = nondimensional test specimen vertical displacement
ξ_{equil} = nondimensional equilibrium position
$\xi_{1,2}$ = initial and peak vertical displacements
ζ = nondimensional beam stiffness
Γ = nondimensional unbalanced spring force
$()'$ = nondimensional time derivative

Received July 11, 1988; revision received Feb. 20, 1989.

*Aerospace Engineer, Spacecraft Dynamics Branch, Structural Dynamics Division. Member AIAA.

Introduction

THE ultimate goal of advanced suspension system research is to simulate flight boundary conditions for ground testing of large flexible space structures. Approximating free-free modes of a test specimen in a 1-g environment requires a very soft suspension system to avoid restraining the vertical and lateral motions of the suspended structure. If springs and/or suspension cables are used, "softness" depends on factors such as suspension length, stiffness, and mass. It is desirable to have suspension frequencies substantially less than the fundamental frequency of the structure being tested, to avoid excessive interactions. For cables, suspension frequency can be lowered by increasing length. However, the size limitations of available test facilities limit the lowest frequency that can be achieved. Also, lateral cable vibration becomes a concern as suspension cable length increases.

Various concepts for low-frequency suspension systems have been proposed for counteracting gravity loads. Dr. E. F. Crawley of the Massachusetts Institute of Technology has surveyed leading candidates, which include constant-volume or constant-pressure pneumatic systems, constant-pressure hydraulic systems, active servo systems, and zero-spring-rate mechanical devices. His survey concluded that the constant-volume pneumatic system and the zero-spring-rate mechanism are the most promising devices to use in ground testing flexible structures when feasibility, complexity, and cost, among other things, are the leading design factors.

Zero-spring-rate mechanisms (ZSRM), such as that shown in Fig. 1, offer promise for reducing the required suspension cable lengths. These mechanisms allow the structure to be supported on relatively short, stiff cables. ZSRMs consist of a linear spring in parallel with two horizontal prestressed (compressed) beams that produce a nonlinear negative vertical stiffness component when deflected. The effective suspension vertical stiffness of the ZSRM, for small motion about the horizontal position of the prestressed beams, decreases to zero as the prestressed load in the beams increases to some critical value. The regime of linear motion decreases as the applied load approaches this critical value. At loads greater than this critical value, the system is unstable about the beam horizontal position. However, nonlinear effects limit deflection above the critical value.

If the ZSRM has a negligible mass and operates in its linear range, an applied critical prestressed load exists at which the system stiffness, and thus the system suspension frequency, becomes zero. However, in practice, the mass and stiffness of the cable cause the system to have a nonzero minimum frequency. In addition, large deflections cause axial unloading

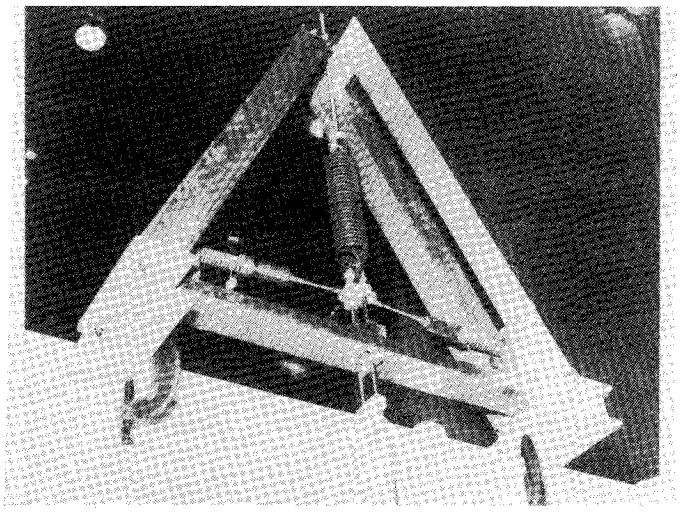

Fig. 1 Zero-spring-rate mechanism.

of the beam members. The unloading also causes the system stiffness to increase. Various ZSRMs have been studied in the range of linear motion.[1-3] However, although they are designed to operate in the linear range, it is important to be able to identify how the system behaves if the motion becomes nonlinear. Imperfections in the system can initiate nonlinear motion, which becomes more pronounced as the effective stiffness of the system decreases. Thus, understanding how the system behaves during the transition from the linear to the nonlinear range and how system imperfections produce nonlinearity are important design factors, particularly at unusually low frequencies.

The objectives of this paper are 1) to present the results of an investigation on the transition between the linear and nonlinear range of motion for the ZSRM suspension system and 2) to characterize nonlinear behavior due to system imperfections. The feasibility of using a nonlinear code, such as the Large Angle Transient Dynamics (LATDYN) computer code,[4] to analyze the behavior of the ZSRM and various suspended test articles is also addressed. The LATDYN computer code uses convected, finite-element transient analysis to accurately treat elastic deformation and large rigid-body motion. The beam elements used in the code are of a consistent mass formulation. A consistent mass formulation of the finite-element equations of motion (rather than a lumped mass formulation) is developed so that exact rotational inertial properties are retained in the analysis. This is critical for structural elements under large rotations. A simple mathematical model of the system renders a closed-form solution when only the vertical motion of the system is considered. This mathematical model is used to validate the code for extension to more complex models.

Analysis

The simplest model for analyzing the dynamic behavior of a ZSRM is to have it suspend a lumped mass via a cable (Fig. 2). This would allow vertical and pendular motion. The linear spring is prestretched to offset the weight of the lumped mass. Ideally, the linear spring should be prestretched until the prestressed beams are perfectly horizontal. If there is an error in this adjustment, the beams will not be perfectly horizontal at equilibrium. The equilibrium position is very sensitive to adjustment error and perturbations from adjustment, particularly if the prestressed loads are large. Instrumentation placed on the suspended specimen after the linear spring had been perfectly prestretched would also result in a new equilibrium position. The mass of the beams are assumed to be substantially less than the suspended lumped mass and can be ignored. The vertical motion and pendular motion about the

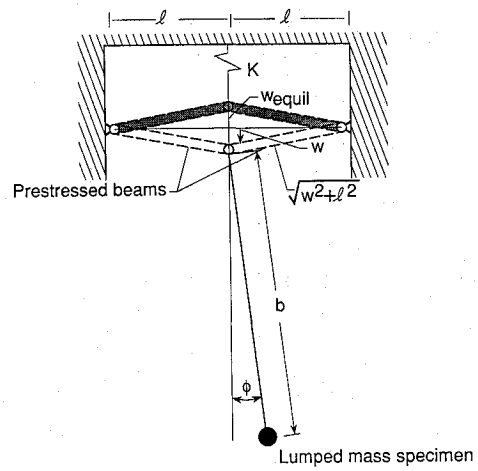

Fig. 2 Zero-spring-rate mechanism suspending lumped mass via a cable.

equilibrium position of the lumped mass is given by Eqs. (1) and (2), respectively,

$$M\ddot{\bar{w}} + K\bar{w} + Mb\ddot{\phi}\sin\phi + Mb\dot{\phi}^2\cos\phi - \frac{2P\bar{w}}{\sqrt{l^2+\bar{w}^2}} + 2EA\bar{w}\left(\frac{1}{l} - \frac{1}{\sqrt{l^2+\bar{w}^2}}\right) = 0 \tag{1}$$

$$Mb^2\ddot{\phi} + Mb\ddot{\bar{w}}\sin\phi + Mgb\sin\phi = 0 \tag{2}$$

where

$$\bar{w} = w - w_{equil}$$

$$M = m_{cable} + m_{specimen}$$

If the weight is not exactly balanced at the horizontal beam position, an unbalanced force Q will be present at this position. This force will shift the equilibrium position away from the horizontal position, thus

$$w_{equil} = w_{equi}(Q)$$

The first two terms of Eq. (1) are those of a spring-mass system. The next two terms are the Coriolis and centripetal terms, respectively. Negative stiffness, which softens the system, is given by the fifth term. This stiffness is proportional to the prestressed beam load and occurs when the beam tips are deflected from their horizontal position. Because the beams are prestressed, axial unloading must also be considered for large deflections. The vertical component of unloading is expressed by the sixth term. The second term in Eq. (2) indicates that if the vertical motion is large, the pendular motion would no longer be that of a simple harmonic oscillator.

Linear Analysis

Linearizing the system, and assuming a massless rigid cable, we have for small vertical and pendular displacements

$$M\ddot{\bar{w}} + (K - 2P/l)\bar{w} = 0 \tag{3}$$

$$Mb^2\ddot{\phi} + Mgb\phi = 0 \tag{4}$$

The linear, vertical, and pendular motions are completely uncoupled. Vertically, the suspended specimen oscillates at a frequency inversely proportional to the prestressed load in the beams.

$$\omega_{resultant} = \sqrt{\frac{K - (2P/l)}{M}} \tag{5}$$

Linearly, there exists a critical load P_c at which $\omega_{\text{resultant}}$ goes to zero. This load is

$$P_c = Kl/2 \tag{6}$$

This analysis is valid for critical loads less than the Euler buckling load of the beams. Without the compressive loads, the system has a natural frequency ω_0

$$\omega_0 = \sqrt{K/M} \tag{7}$$

The linear spring and the negative spring created by the beams act in parallel. This combination is in series with the cable. Thus, the system effective frequency including the mass and stiffness of the cable is

$$\omega_{\text{eff}} = \sqrt{\frac{K_{\text{cable}}(K + K_{\text{neg}})}{M(K + K_{\text{neg}} + K_{\text{cable}})}} \tag{8}$$

with K_{neg} and K_{cable} being the stiffness of the prestressed beams and cable, respectively.

Nonlinear Analysis

If the pendular effects are neglected, the equation of the vertical motion about the horizontal beam position becomes

$$M\ddot{w} + (K + 2EA/l)w - \frac{2(P + EA)w}{\sqrt{l^2 + w^2}} = Q \tag{9}$$

The nonlinear load-deflection curves are illustrated in Fig. 3 for various prestressed load-critical load ratios. In the absence of Q, they provide a means for determining the operating range of the ZSRM. This range is the linear portion of the curves with positive slopes (i.e., $P/P_c < 1.0$) near the origin. Prestressed loads greater than the critical load would make the system unstable. Therefore, to minimize the suspension frequency, it is necessary to have the prestressed load near but not exceeding the critical load.

To generalize the results, nondimensional variables will be used. Nondimensionalizing time as

$$\bar{t} = \omega_0 t$$

and vertical displacement as

$$\xi = w/l$$

results in

$$\dot{\xi} = \omega_0 \xi' \quad \text{and} \quad \ddot{\xi} = \omega_0^2 \xi''$$

where

$$()' = \frac{\mathrm{d}()}{\mathrm{d}\bar{t}}$$

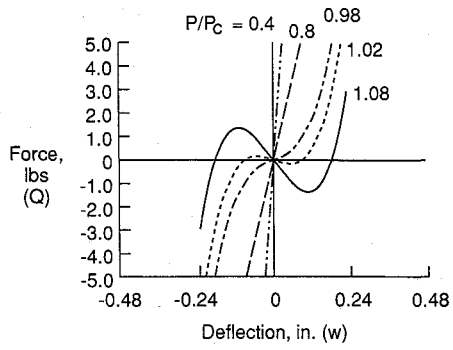

Fig. 3 Nonlinear load-deflection diagram of ZSRM.

Letting

$$\zeta = \frac{2EA}{Kl}, \quad \bar{P} = \frac{2P}{Kl}, \quad \text{and} \quad \Gamma = \frac{Q}{Kl}$$

the nondimensional equation of vertical motion is

$$\xi'' + (1 + \zeta)\xi - \frac{(\bar{P} + \zeta)\xi}{\sqrt{1 + \xi^2}} = \Gamma \tag{10}$$

Nondimensionally, the system velocity is

$$\eta = \frac{\mathrm{d}\xi}{\mathrm{d}\bar{t}}$$

Separating variables η and ξ, the equation of motion is integrated to give the system energy equation

$$\eta^2 + (1 + \zeta)\xi^2 - 2(\bar{P} + \zeta)\sqrt{1 + \xi^2} - 2\Gamma\xi = h \tag{11}$$

When we use a Taylor series expansion on the radical

$$\sqrt{1 + \xi^2} \approx 1 + \frac{\xi^2}{2}$$

The nondimensional energy equation becomes

$$\eta^2 + (1 - \bar{P})\xi^2 - 2\Gamma\xi = \bar{h} \tag{12}$$

where

$$\bar{h} = h + 2(\bar{P} + \zeta) \tag{13}$$

There are two positions of maximum potential energy when the velocity is zero, ξ_1 and ξ_2, where

$$\xi_{1,2} = \frac{\Gamma \pm \sqrt{\Gamma^2 + (1 - \bar{P})\bar{h}}}{(1 - \bar{P})} \tag{14}$$

The dimensional positions are

$$w_{1,2} = \frac{Ql \pm l\sqrt{Q^2 + (K/2 - P/l)(2(P + EA)l + H)}}{(Kl - 2P)}$$

where H is the system total energy. The equilibrium position is the average of the maximum potential energy positions, hence

$$\xi_{\text{equil}} = \Gamma/(1 - \bar{P}) \tag{15}$$

or, dimensionally as

$$w_{\text{equil}} = Q/(Kl - 2P)$$

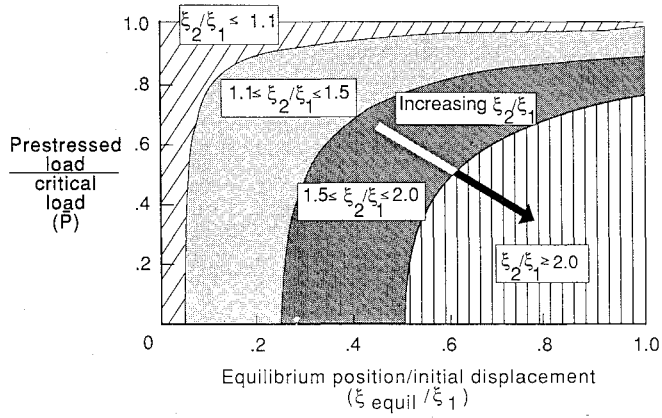

Fig. 4 Nonlinearity dependence upon prestressed load, initial displacement, and equilibrium position.

Table 1 ZSRM and cable properties

Prestressed aluminum beams	
Length	12.0 in.
Diameter	1.0 in.
Wall thickness	1/16 in.
Modulus of elasticity	10.5×10^6 psi
Mass density	0.003037 slugs/in.^{3}
Euler buckling	14620.0 lb
Critical load	1462.0 lb
Stainless steel cable	
Length	30.0 ft
Diameter	1/16 in.
Modulus of elasticity	30.0×10^6 psi
Mass density	0.0089 slugs/in.^{3}
Spring	
Spring constant	243.7 lb/in.
Spring length	3.28 ft

With the linear spring perfectly adjusted, the motion of the lumped mass would be linear. The lumped mass would oscillate with an amplitude equal to that of its initial displacement. The horizontal beams could be prestressed to the critical load, thereby minimizing the suspension system frequency. However, with an error in the adjustment, the equilibrium position would shift. The lumped mass would oscillate between two positions. One of these positions would be its initial displacement. The other would depend on the unbalanced force at the horizontal beam position and the prestressed load in the beams. The motion would be nonlinear because the amplitude of oscillation is greater than the initial displacement, or

$$\xi_2/\xi_1 > 1.0$$

The nonlinearity is proportional to the shift in the equilibrium position and the prestressed load in the beams. Each combination of prestressed load and equilibrium position produces a unique ξ_2/ξ_1 ratio. The nonlinearity that results from shifting the equilibrium position is illustrated in Fig. 4 for various equilibrium position-prestressed load combinations. For example, a prestessed critical-load ratio of 0.4 and equilibrium initial-position ratio of 0.4 would result in ξ_2/ξ_1 ratio in the region of $1.1 < \xi_2/\xi_1 < 1.5$. As the system is softened (i.e., as $P \rightarrow P_c$) the motion could become large compared to its initial displacement. Here we are using a lumped mass, but when the test specimen is very flexible, the large motion could potentially damage the test specimen.

Numerical Results

The numerical results presented in this section address the feasibility of using a nonlinear computer code such as LATDYN to analyze the dynamic behavior of more complex suspension configurations (i.e., suspending flexible structures). The closed-form solution of the vertical motion is used to validate the numerical results generated by LATDYN for extension to these configurations. Pendular motion is examined to ascertain its effects on vertical motion for various sets of initial conditions. Table 1 contains the physical properties of the ZSRM used for the following results.

The ZSRM properties are based on the prestressed beam's Euler buckling load. The critical load can be any load less than the buckling load. Spring stiffness is specified such that the resultant frequency is zero when the prestressed load equals the critical load. Suspension frequency, spring stiffness, and Euler buckling load depend on the prestressed beams' cross-sectional area and length. The spring supports a 44-lb mass.

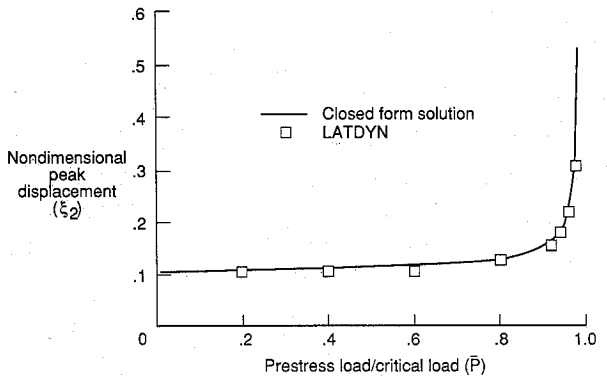

Fig. 6 Peak displacement variation with prestressed load.

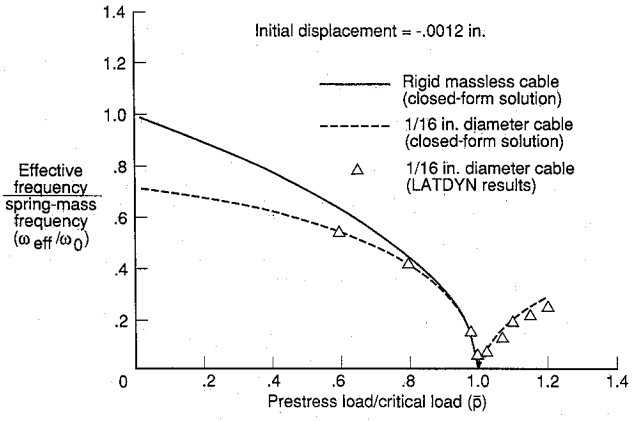

Fig. 7 Frequency variation with prestressed load.

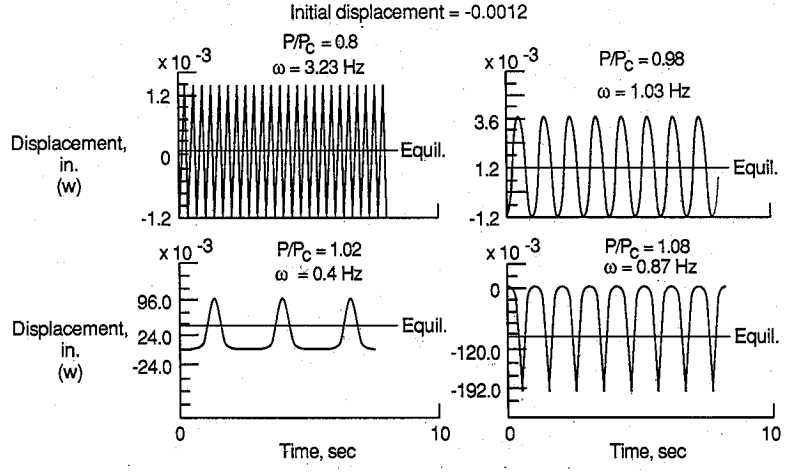

Fig. 5 Suspended lumped-mass vertical displacement.

Parametric studies were conducted in which prestressed load was varied to study the effect on system frequency. The vertical displacements of the suspended mass are illustrated in Fig. 5 for load ratios P/P_c of 0.8, 0.98, 1.02, and 1.08. The lumped mass was given an initial downward displacement of 0.0012 in. As the load is increased, the equilibrium position is shifted further away from the desired horizontal beam position with the motion becoming more nonlinear. All the load ratios have peak displacements above the horizontal beam position except for $P/P_c = 1.08$. At this value, the beams collapse until the linear spring pulls them back up. The nondimensional peak displacement (ξ_2/ξ_1) variation with prestressed load is illustrated in Fig. 6. Although nonlinear for all the prestressed loads, the nonlinearity becomes more pronounced for load ratios greater than $P/P_c = 0.9$. The frequency is reduced as the load increases until it reaches some minimum value as shown in Fig. 7. Loads greater than this value cause the frequency to increase. Also, Figs. 6 and 7 show that the results from LATDYN agree with those generated from the closed-form solution.

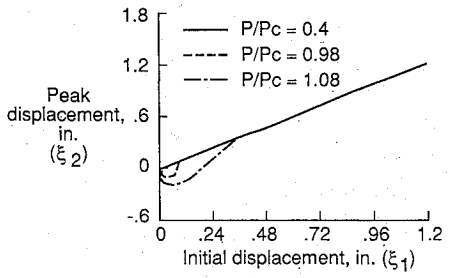

Fig. 8 Initial displacement effects on peak displacement.

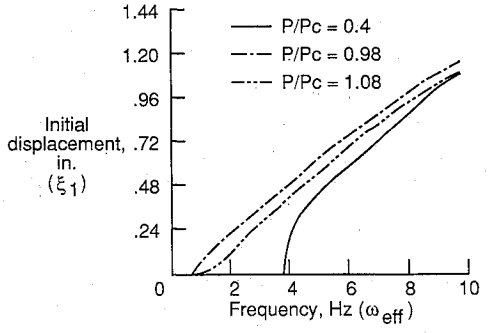

Fig. 9 Initial displacement variations with frequency.

Frequency and peak displacement are affected by initial displacement of the lumped mass. Figure 8 shows the peak displacement variation within initial displacement for various load ratios. As the initial displacement increases, the curves become more linear. The curves for the higher load ratios are more nonlinear because the equilibrium position is dependent upon the prestressed load. Because the equilibrium shift is independent of initial displacement, the nonlinear effects of shifts in the equilibrium position are more pronounced for smaller initial displacements. Figure 9 illustrates how initial displacement influences the suspension system frequency. In linear systems, frequency is independent of initial displacement. The smaller initial displacements in Fig. 9 yield frequencies approximately equal to those of the linear system. For very small displacements, the frequency decreases as the load ratio increases even as the load increases past the critical load. However, the instability at loads above the critical load would not permit operation in this range.

The aforementioned results depict the system dynamics when only vertical motion is assumed. If the suspended test article is given a sufficiently large initial horizontal displacement, pendular motion results as well. For $P/P_c = 0.8$, two cases of initial conditions were considered. In the first case, the suspension system beam tips are given the same initial downward deflection as the suspended mass. The pendular motion is superimposed on the vertical motion of the system as shown in Fig. 10. When the beam tips are deflected substantially less than the mass, only the pendular motion is discernible. These results are the same for $P/P_c = 1.02$.

Concluding Remarks

The ability of zero-spring-rate mechanisms to reduce the natural frequency of cable suspension systems in ground vibration tests has been examined for linear and nonlinear effects. A closed-form solution to the dynamic model of the system predicted system behavior that could not be gained from static stability analysis based on a force-deflection diagram. The code provided insight into the analysis and some of the numerical results shown in the paper. The closed-form solution predicted that an imperfection in the linear spring prestretch would shift the equilibrium position of the vertical motion. This equilibrium shift resulted in the system having peak displacements, which grew in magnitude with imperfec-

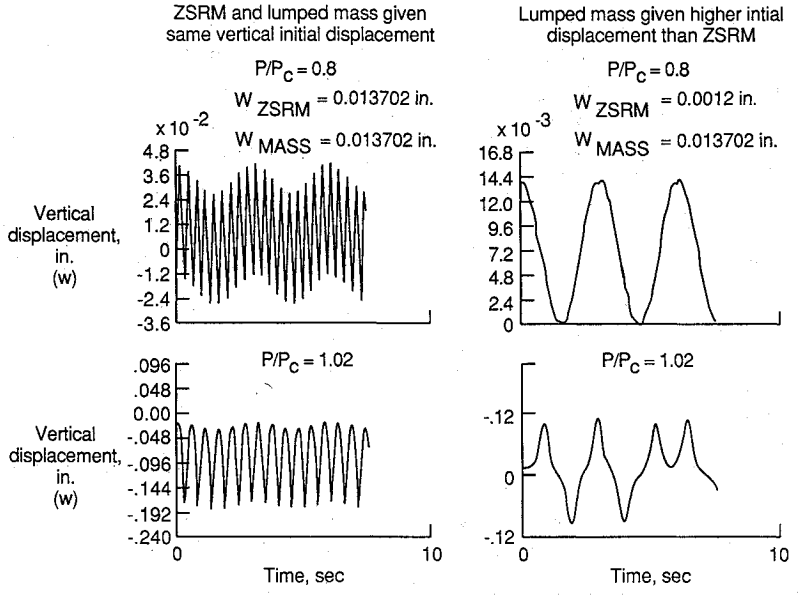

Fig. 10 Nonlinear pendular motion of lumped mass.

tion and applied prestressed load. Dependency of the nonlinear vertical displacements on prestressed load, prestretch imperfection, and initial displacement has been determined. Large horizontal initial deflections result in pendular motion, which couples with vertical motion. The agreement of results produced by the closed-form solution and the nonlinear multibody computer code to model the dynamics of a zero-spring-rate mechanism and lumped mass being suspended by it demonstrates that the multibody code can be used to model more complex systems.

Future analytical and experimental work in analyzing zero-spring-rate mechanisms should consider the damping effects of the mechanism.

References

[1]Gayman, W. H., Trubert, M. R., Abbott, P. W., "Measurement of Structural Transfer Functions Significant to Flight Stability of the Surveyor Spacecraft," NASA TM 33-389, May 1969.

[2]Rogers, L. C., and Richards, K. E., "PACOSS Program Overview and Status," First NASA/Dept. of Defense Control/Structures Interaction Technology Conference, Norfolk, VA, Nov. 1986.

[3]Gold, R. R., and Reed, W. H., "Preliminary Evaluation of Suspension Systems for 60-Meter Mast Flight System," NASA Langley Research Center, Rept. C2602-008, Feb. 1987.

[4]Housner, J. M., McGowan, P. E., Abrahamson, A. L., and Powell, M. G., "The Latdyn User's Manual," NASA TM 87635, Jan. 1986.